J. Phys. Chem. **1996,** *100,* 1827−1832 **1827**

Stereochemical Effects on Monolayer Formation of $[Ru(dpp)_3]^{2+}$ (dpp = 4,7-Diphenyl-1,10-phenanthroline) at an Air−Water Interface

Akihiko Yamagishi,* Yasutomo Goto, and Masahiro Taniguchi

Division of Biological Sciences, Graduate School of Science, Hokkaido University, Sapporo 060, Japan

Received: July 31, 1995; In Final Form: October 19, 1995[⊗]

Stereochemical effects on monolayer formations have been studied at an air−water interface for the racemic mixture and enantiomer of $[Ru(dpp)_3](ClO_4)_2$ (dpp = 4.7-diphenyl-1,10-phenanthroline). Stearic acid (SA) was added to reduce the cohesive interaction of the Ru(II) complexes. The ratio of SA to Ru(II) complex, [SA]/[Ru], was varied from 0 to 4. At [SA]/[Ru] = 0 and 1, the "lift-off" area per molecule at which the surface pressure increased from zero was smaller for the racemic mixture than for the enantiomer. The results indicated that the racemic mixture of the Ru(II) complex formed a more compact monolayer than the enantiomer. There was no difference observed in the surface pressure−molecular area ($\pi-A$) curves at [SA]/[Ru] larger than 3. The monolayer was transferred onto a hydrophobic glass or silicon wafer substrate as a Langmuir−Blodgett (LB) film of Y-type. At [SA]/[Ru(II)] = 1, the $d(001)$ spacing of the film was determined by X-ray diffraction measurements, leading to $d(001)$ = 50.4 and 37.8 Å for the racemic mixture and the enantiomer, respectively. The IR reflection−absorption spectroscopy showed that the alkyl chains of SA molecules took different orientations for the racemic and enantiomeric films. It is postulated that SA molecules which intervened between the Ru(II) complexes are more perpendicular to the substrate surface due to the closer packing of the racemic Ru(II) complexes than the enantiomers.

Introduction

Recently the Langmuir−Blodgett (LB) films of metal complexes have been investigated extensively with the purpose of developing functional materials for sensors, electrode-modifiers, nonlinear optical devices, and pyroelectric materials.[1−6] The electronic and magnetic properties of metal complexes are intended to be utilized to achieve these functions. In these attempts, it is of vital importance to clarify the packing structures of surfactant metal complexes on a two-dimensional surface. It is of value to establish the relationship between the molecular arrangements and the stereochemical properties of the component molecules.

When optical isomers form a monolayer at an air−water interface, they are expected to be mixed uniformly on a molecular scale because their steric and electronic properties are the same except for the absolute configurations. In some cases, however, the isomers are separated into two homochiral phases.[7] Such systems provide an ideal binary system to investigate the mixing and packing structures of two different kinds of molecules. There have been a number of investigations reported on the monolayer and LB film formations of chiral organic molecules.[8−12] As far as we know, however, no attempts have been reported on the chirality effects of metal complexes on monolayer formation.

In the present work, we report the stereochemical effects on the monolayer formation of an optically active metal complex, $[Ru(dpp)_3]^{2+}$ (dpp = 4.7-diphenyl-1,10-phenanthroline), at an air−water interface. We compare the monolayer and LB film properties between the racemic mixture and the pure enantiomer of the metal complex. The monolayer behaviors of racemic $[Ru(dpp)_3]^{2+}$ were investigated previously.[13] This complex has been chosen because it has a remarkable geometrical structure in the periphery region (Figure 1). Two phenyl rings in each ligand project out from the central metal ion, and as a consequence, the optical isomers are expected to interact with each other in a highly stereoselective way.

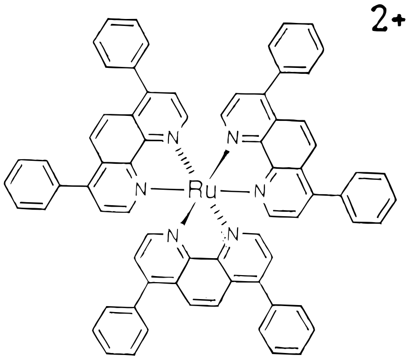

Figure 1. Structure of $[Ru(dpp)_3]^{2+}$.

Experimental Section

Materials. $[Ru(dpp)_3](ClO_4)_2$ (dpp = 4,7-diphenyl-1,10-phenanthroline) was prepared by refluxing $K_2[Ru(H_2O)Cl_5]$ (0.5 g) with dpp (2.0 g) in 20 mL of a 1:1 water−ethanol (v/v) solution for 12 h. The reactant was reduced by adding 1.2 mL of hypophosphorous acid, and then the mixture was refluxed further for 2 h. An orange precipitate was formed by adding $NaClO_4$ to the reactant mixture. Resolution of $[Ru(dpp)_3]^{2+}$ was performed by adding 0.1 g of sodium antimonyl tartrate to 20 mL of a 1:1 water−ethanol (v/v) solution of the racemic mixture. Δ-$[Ru(dpp)_3]^{2+}$ was filtered off as an insoluble antimonyl tartrate salt. The anion of the salt was converted to the perchlorate by use of an anion-exchange resin. Λ-$[Ru(dpp)_3](ClO_4)_2$ was obtained by adding an excess amount of sodium perchlorate to the filtrate. The optical purity of each isomer was checked in the ^{1}H-NMR spectrum by use of tris[3-((heptafluoropropyl)hydroxymethylene)-(+)-caphorato]europium(III) derivative (Aldrich Chemical Co.) as a chiral shift reagent. The optical purities of both enantiomers were estimated to be

---

* To whom correspondence should be addressed.

[⊗] Abstract published in *Advance ACS Abstracts,* January 1, 1996.

0022-3654/96/20100-1827$12.00/0

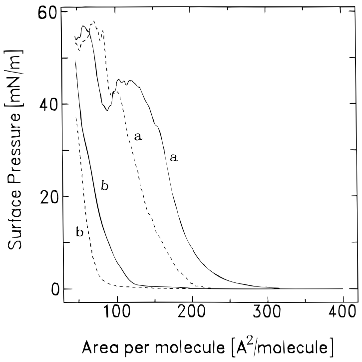

Figure 2. π−A curves of [Ru(dpp)$_3$](ClO$_4$)$_2$ at 20 °C. The subphase is 0.1 M NaClO$_4$. Solid and dotted curves are the enantiomer and racemic mixture, respectively. Curves a are the results at the initial compression experiments; curves b, the results when the initially compressed layers were expanded and compressed again.

higher than 95%. The CD spectra of δ and λ enantiomers gave 324 and −330 as $\Delta\epsilon$ at 281 nm, respectively. The solubility of racemic or enantiomeric [Ru(dpp)$_3$](ClO$_4$)$_2$ was estimated to be less than 10^{-7} M in water. Stearic acid (SA) was purified by recrystallization from a 1:1 (v/v) chloroform−hexane solution. A hydrophobic glass substrate was prepared by treating a quartz glass plate with a toluene solution of trimethylmonochlorosilane. Other reagents were used as purchased. Water was deionized with a Milli-Q SP reagent water system (Millipore) to a specific resistivity of 18.4 MΩcm).

Instruments. A surface pressure versus area per molecule (π−A) curve was obtained with a Langmuir trough and a Joyce−Loeble monolayer coating unit with a Whilhelmy balance. A chloroform solution of the Ru(II) complex and SA was spread over an aqueous 0.1 M NaClO$_4$ solution at 20 °C. The rate of compression was 90 cm^2/min. A LB film was prepared by a vertical dipping method by transferring a monolayer to a hydrophobic glass or silicon wafer substrate at the dipping rate of 4 mm/min. The transfer ratio was close to unity for both downward and upward directions, confirming the formation of a Y-type film. An X-ray diffraction pattern was recorded with an X-ray diffractometer (Rigaku Co., Japan) at the wavelength of CuK (1.540 56 Å) under the conditions of 40 kV and 30 mA. The reflection−absorption IR spectrum of a LB film deposited on a silicon wafer was measured with a FT-IR spectrometer, JIR-7000 (JEOL, Japan) at the incident angle of 85°. An electronic absorption spectrum was obtained with a spectrophotometer, UVIDEC (JASCO, Japan).

Results

A. Monolayer Behavior. The results of the surface pressure−molecular area curves are shown in Figure 2 when a chloroform solution of pure [Ru(dpp)$_3$](ClO$_4$)$_2$ was spread on an aqueous solution of 0.1 M NaClO$_4$. For Δ-[Ru(dpp)$_3$](ClO$_4$)$_2$ (solid curve a), surface pressure (π) increased from zero at 300 Å^2/molecule (denoted by "lift-off area" of A_1) to a detectable value and reached a maximum of 45 mN/m at 100 Å^2/molecule. When another compression experiment was repeated again on a fresh sample, the same curve was obtained until the surface pressure reached 40 mN/m. The curve was not reproducible, however, above a surface pressure of 40 mN/m. For racemic [Ru(dpp)$_3$](ClO$_4$)$_2$ (dotted curve a), π increased from zero at A_1 = 210 Å^2/molecule, a value appreciably smaller than for the enantiomer. It reached a maximum of 58 mN/m at 70 Å^2/molecule after passing though a region of a small plateau around 100 Å^2/molecule. The reproducibility of a curve was also limited in the region of surface pressure less than 40 mN/m.

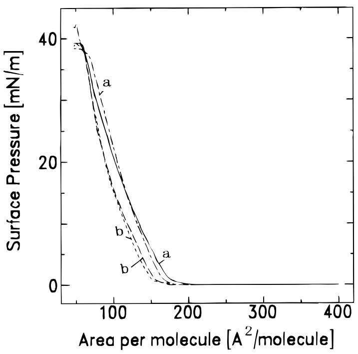

Figure 3. π−A curves of [Ru(dpp)$_3$](ClO$_4$)$_2$ at 20 °C. The conditions were the same as in Figure 1 except that stearic acid (SA) was incorporated at the ratio [Ru]/[SA] = 1. Curves a are the initial (—) and second (30 min later) (− • −) compression results for the enantiomeric ruthenium(II) complexes, respectively. Curves b are the initial (- - -) and second (30 minute later) (• • •) compression results for the racemic mixture of the ruthenium(II) complexes, respectively.

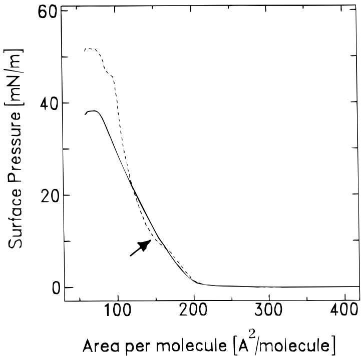

Figure 4. π−A curves of [Ru(dpp)$_3$](ClO$_4$)$_2$ at 20 °C at the ratio [Ru]/[SA] = 2. The other conditions were the same as in Figure 3. Solid and dotted curves are the enantiomer and racemic mixture, respectively.

Curves b in Figure 2 are the results when compression was repeated 1 h after the surface was compressed up to 60 mN/m and expanded again to its initial area. Solid and dotted curves b are for Δ and racemic [Ru(dpp)$_3$]$^{2+}$ samples, respectively. As shown in Figure 2, π remained at zero until the surface was compressed to 120 and 80 Å^2/molecule for the δ enantiomer and racemic mixture, respectively. [Ru(dpp)$_3$](ClO$_4$)$_2$ was insoluble in the present subphase (0.1 M NaClO$_4$). Thus, the decrease of A_1 at the second compression experiment was ascribed to the irreversible formation of microcrystallites during the initial compression.[13] Once the crystallites were formed at higher surface pressure, they did not disperse to isolated molecules even after the surface was again expanded.

With the goal of obtaining a monolayer of [Ru(dpp)$_3$](ClO$_4$)$_2$ with reversible compressibility, stearic acid (SA) was added to a chloroform solution of [Ru(dpp)$_3$](ClO$_4$)$_2$.[14] Curves a and b in Figure 3 denote the results when the chloroform solution was spread at the ratio of SA to the Ru(II) complex (denoted by [SA]/[Ru]) of 1 for the Δ and racemic complexes, respectively. Nearly reproducible π−A curves were recorded for both systems when the curves were measured 30 and 60 min after the initial experiments. A_1 was found to be 150 ± 5 and 170 ± 10 Å^2/molecule for the racemic mixture and the Δ enantiomer, respectively. The results indicated that the racemic mixture occupied a smaller area per molecule than the enantiomer even in the presence of an equal molar amount of stearic acid. Figures 3, 4, and 5 are the results for [SA]/[Ru] = 2, 3, and 4, respectively. Differences in the π−A curves between the enantiomer and racemic mixture were still observed for [SA]/[Ru] = 2, but they disappeared for [SA]/[Ru] = 3 and 4.

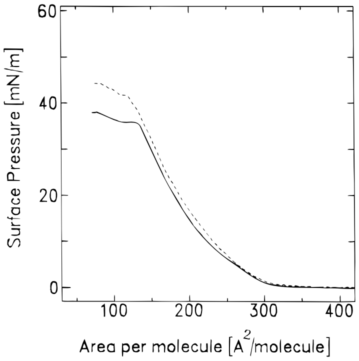

Figure 5. $\pi-A$ curves of $[Ru(dpp)_3](ClO_4)_2$ at 20 °C at the ratio [Ru]/[SA] = 3. The other conditions were the same as in Figure 3. Solid and dotted curves are the enantiomer and racemic mixture, respectively.

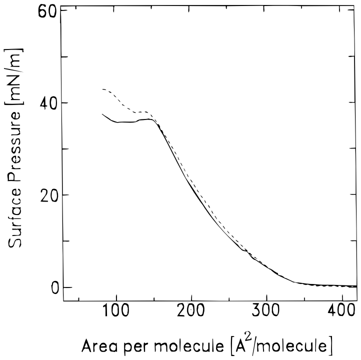

Figure 6. $\pi-A$ curves of $[Ru(dpp)_3](ClO_4)_2$ at 20 °C at the ratio [Ru]/[SA] = 4. The other conditions were the same as in Figure 3. Solid and dotted curves are the enantiomer and racemic mixture, respectively.

One interesting aspect was that a small reflection existed in the $\pi-A$ curve of the racemic sample at [SA]/[Ru] = 2 around the surface pressure of 10 mN/m (indicated by an arrow in Figure 4). No such reflection was observed for the enantiomeric sample. This indicates that the racemic monolayer underwent some phase transition during the compression process. Because the enantiomeric monolayer did not show such a transition, the transition must be related to the stereochemical packing modes of the metal complex.

The effects of temperature were investigated at [SA]/[Ru] = 1 from 10 to 35 °C. It was concluded that temperature changes had little influence on the monolayer behaviors of the present samples.

B. X-ray Diffraction Analyses of the LB Films. X-ray diffraction paterns were obtained for the LB films (50 layers) transferred onto a hydrophobic quartz at 25 mN/m under the conditions of Figures 3−6. The upper and lower parts of Figure 7 show the results for the racemic mixture and the enantiomer at [SA]/[Ru] = 1, respectively. The LB film of the racemic mixture gave sharper diffraction peaks than that of the Δ enantiomer, suggesting a more regular spacing of the layers in the racemic mixture. The peaks at $2\theta = 1.75°$ and 5.46° for the racemic sample were assigned to the $d(001)$ and $d(003)$ diffractions, respectively. The peaks at $2\theta = 2.34°$ and 4.70° for the enantiomeric sample were assigned to the $d(001)$ and $d(002)$ diffractions, respectively. From the $d(001)$ values, the interlayer distance was calculated to be 50.4 and 37.8 Å for the racemic and enantiomeric metal complexes, respectively. These values are compared to the interlayer distance of a LB film of stearic acid alone of 39.7 Å.[15] Table 1 summarizes the basal spacings of the LB films for [SA]/[Ru] = 1−3. The basal spacing for the racemic mixture was smaller than that for the enantiomer at [SA]/[Ru] = 1. The former decreased with the increase of [SA]/[Ru], while the latter increased with an increase in [SA]/[Ru] until they were almost identical at [SA]/[Ru] = 3.

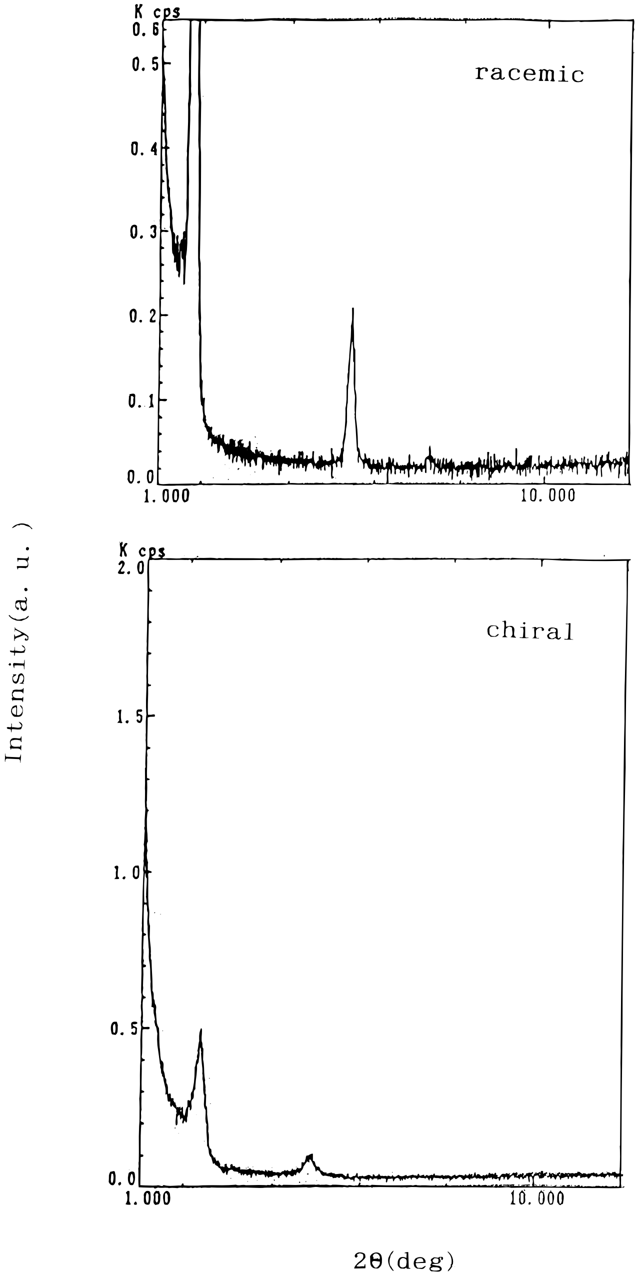

Figure 7. X-ray diffraction patterns of the films of $[Ru(dpp)_3](ClO_4)_2$ and stearic acid at [Ru]/[SA] = 1. The film was deposited on a hydrophobic glass substrate to 50 layers: (upper) racemic mixture and (lower) enantiomer.

TABLE 1: Basal Spacings of LB Films of Racemic and Enantiomeric $[Ru(dpp)_3]^{2+}$ (Ru) and Stearic Acid (SA)

ratio of [SA] to [Ru]	racemic mixture (Å)	enantiomer (Å)
1:1	50.4	37.8
2:1	48.7	38.9
3:1	38.4	39.4

C. UV and IR Spectral Analyses of the LB Films. The electronic absorption spectrum was measured for 50 layers of a LB film deposited on a quartz substrate. In the measuremts, unpolarized light was perpendicularly incident on the samples. Figure 8 shows the spectra of the racemic and Δ complexes at [SA]/[Ru] = 1. It is seen that the absorbance peak was observed at 480 nm due to the metal-to-ligand charge transfer band of $[Ru(dpp)_3]^{2+}$. The position was nearly the same as observed in a chloroform solution (482 nm). The intensity of the peak

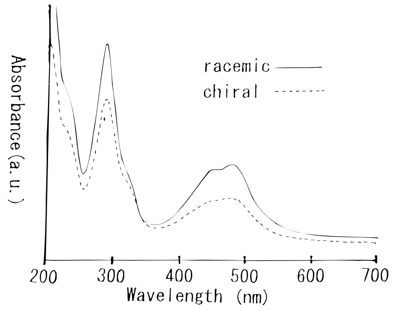

Figure 8. Electronic absorption spectra of the films of $[Ru(dpp)_3](ClO_4)_2$ and stearic acid at [Ru]/[SA] = 1. The film was deposited on a glass substrate to 50 layers: (solid) racemic mixture and (dotted) enantiomer.

is about 2 times higher for the racemic film than for the enantiomeric film, leading to the conclusion that the surface density of the Ru(II) complex was higher for the racemic sample than for the enantiomer sample when the monolayers were deposited at the same surface pressure (20 mN/m). This was coincident with the higher packing of the former as deduced from the $\pi-A$ curves (Figure 3).

IR reflection−absorption spectra were measured for 100 layers LB films deposited on a silicon wafer at [SA]/[Ru] = 1. Parts a and b of Figure 9 are the spectra of the Δ and racemic films, respectively. It is noted that the intensity of the doublet at 2800−2900 cm^{-1} was much higher than that of the singlet at 1100 cm^{-1} for the enantiomeric film, whereas the former was lower than the latter for the racemic film. The doublet peaks at 2923 and 2854 cm^{-1} were assigned to the asymmetric and symmetric stretching vibrations of the methylene groups of SA, respectively.[16] The singlet at 1106 cm^{-1} was assigned to the out-of-plane bending vibration of the CH group of the dpp ligands of $[Ru(dpp)_3]^{2+}$. Because the transfer ratios were close to unity in both samples, the enantiomeric and racemic films contained equal amounts of SA and the metal complex. Thus, the intensity difference in the above spectra implied that the CH_2 groups in SA and the CH groups in the metal complex take up different orientations in the enantiomeric and racemic films. As a comparison, the transmission spectra were recorded on the cast samples of the chloroform solutions (Figure 10a,b). In both of the samples, the doublet at 2800−2900 cm^{-1} had higher intensity than the singlet at 1106 cm^{-1}. The interpretation of the results will be given in the Discussion section.

Discussion

The effects of homo- and heterochirality on monolayer formation have been investigated extensively.[8−12] The works are concerned with organic surfactant molecules such as the amino acid molecules derivatized by long alkyl chains. The chirality of a molecule is due to the asymmetric carbon atoms. In these cases, the stereochemical effects on molecular packing are caused by the interactions among the functional groups such as carbonyl, amine, and hydroxyl groups. The orientations of these functional groups play an essential role in determining the molecular packing in a monolayer state.

In contrast to the earlier studies, the present work is focused on the effects of the helical coordination structure in a tris-chelated complex. A complex of this type has notable asymmetry especially when it possesses bulky planar ligands.[17] In the packed states, the steric interactions between the ligands of neighboring molecules affect the efficiency of molecular packing remarkably. In fact, the crystal structure of a chiral tris-chealted complex is dependent on the homo- and heterochilarity.[18−20]

The complex studied in the present work, $[Ru(dpp)_3]^{2+}$, has six phenyl groups at the periphery region of the phenanthroline ligands (Figure 1). These groups are expected to cause a stereochemical effect when the complex interacts sterically with its neighboring molecules. From the curves of the surface pressure−molecular surface area, the monolayers collapse at a surface pressure less than 40 mN/m irrespective of the presence of stearic acid (SA). This indicates that the monolayers are stable only when they form a liquid-like packing structure. When the ratio of incorporated SA is high enough, the monolayer is expected to approach a solid-like state in which the long alkyl chains are packed to form a crystalline-like ordered array.[14]

We note that there exists a definite difference in the surface pressure−area curves between the enantiomeric and racemic mixture of $[Ru(dpp)_3]^{2+}$ when the ratio of SA to the complex, [SA]/[Ru], is varied from 0 to 2. One result is that the lift-off area, A_1, at which the molecules start to interact sterically is smaller for the racemic mixture than for the enantiomer at [SA]/[Ru] = 1. It is concluded that the monolayer of the racemic mixture attains closer packing than that of the pure enantiomer even in a liquid-like state. The difference between the racemic mixture and the enantiomer is largest in the pure metal complex and decreases with an increase in the fraction of the incorporated SA molecules. The pure metal complexes, however, do not form a reversible monolayer film. It is previously reported that

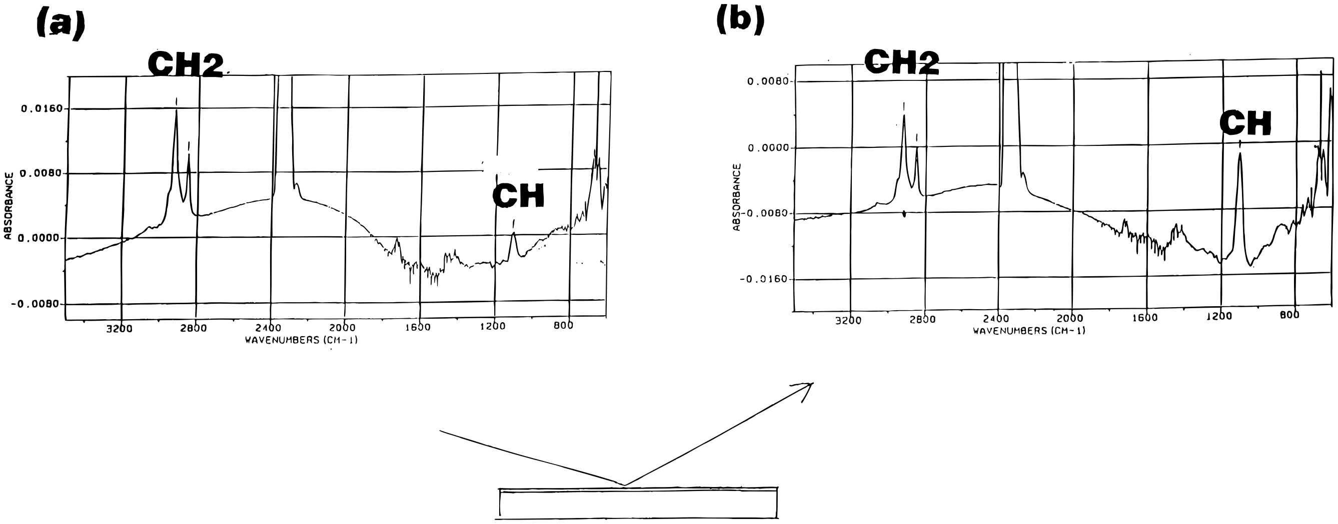

Figure 9. Reflection−absorption IR spectra of the films of $[Ru(dpp)_3](ClO_4)_2$ and stearic acid at [Ru]/[SA] = 1. The film was deposited on a silicon substrate to 100 layers: (a) racemic mixture and (b) enantiomer. The light was incident on the film at an angle of 85°.

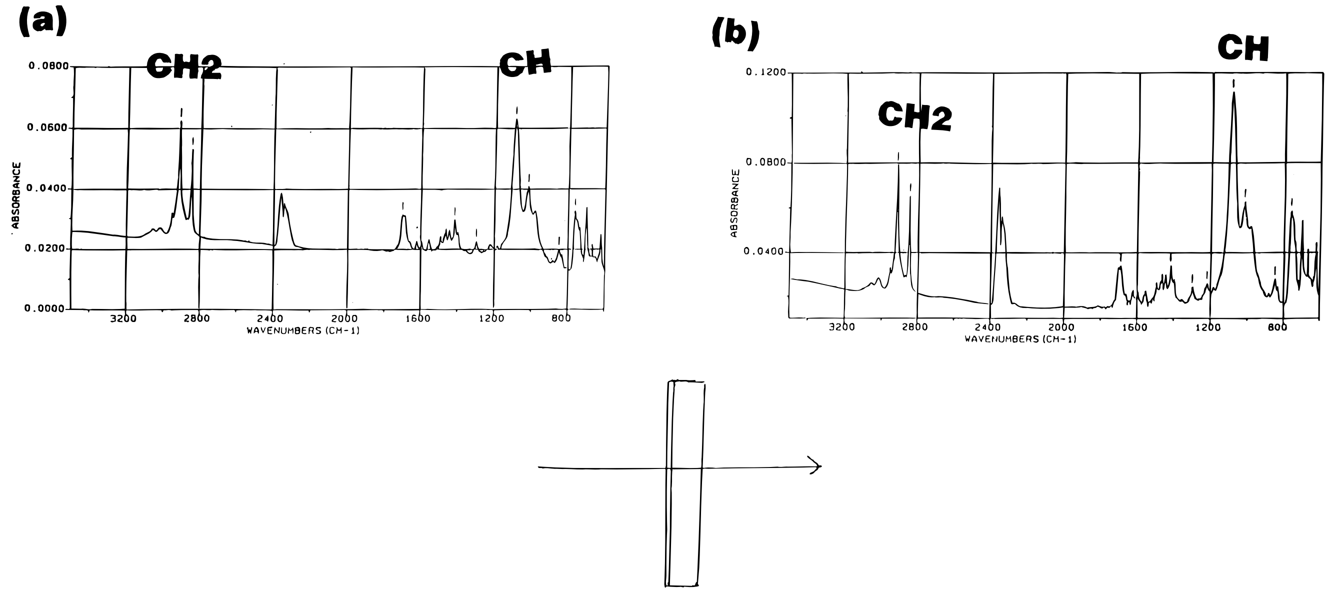

Figure 10. Absorption IR spectra of the cast films of $[Ru(dpp)_3](ClO_4)_2$ and stearic acid at [Ru]/[SA] = 1. The film was cast on a silicon substrate as a chloroform solution under the same conditions as in Figure 9: (a) racemic mixture and (b) enantiomer.

$[Ru(dpp)_3]^{2+}$ irreversibly forms a microcrystallite at an air−water interface when the monolayer is compressed.[13]

According to a space-filling molecular model, $[Ru(dpp)_3]^{2+}$ occupies an area of about 300 Å^2 (denoted by the theoretical limiting area) when it rotates freely on a water surface. In the absence of SA, A_1 for the enantiomer almost coincides with the theoretical limiting area, whereas A_1 for the racemic mixture is much smaller than the model value (300 Å^2). Thus, the enantiomers repel each other at the distance at which the molecules are in contact with each other, whereas the racemic mixture forms a more dense monolayer, probably with the phenyl groups of the facing ligands stacked closely together. Interestingly enough, as the SA molecules are incorporated at the ratio of [SA]/[Ru] = 1, A_1 is smaller than the above theoretical limitting area for both enantiomeric and racemic complexes. This decrease is understood through the assumption that the association of SA molecules reduces the steric interaction between the metal complexes, leading to closer stacking. Most probably the SA molecules are located in the narrow spaces between the phenyl groups. It has been reported that alkyl chains enhance attractive interactions with the aromatic groups.[21] Even in the presence of the SA molecules, the racemic mixture still attains higher packing states than the enantiomer.

In a crystalline state, a tris(acetylacetonato)complex, $[Cr(acac)_3]$ or $[Ru(acac)_3]$, has its planar ligands facing closely the ligands of its neighboring molecules.[19,20] In a racemic mixture, a homochiral column, in which the molecules are stacked with their C_3 axes on the same straight line, is formed.[18] The columns composed of the Δ and Λ complexes are arranged in an alternative way. In contrast to this, no such close packing is observed in the enantiomeric crystal,[19,20] in which the complexes are associated along the C_2 axes. Although we did not observe the molecular arrangements of the monolayers directly, we expect that similar stacking is achieved in the monolayers of the racemic and enantiomeric complexes. The recent theoretical calculations on the phase diagram of the monolayers of chiral tripodal-shaped molecules predict that the molecules attain higher stacking when they interact mainly through a van der Waals interaction.[22]

The X-ray diffraction results show that the spacing of the LB film of the racemic mixture is larger than that of the enantiomer at [SA]/[Ru] = 1 and 2 (Table 1). These results were in agreement with the monolayer behaviors, as stated above. The results of the IR spectra indicate that the orientation of the alkyl group of SA differs between the racemic and enantiomeric films. According to theory,[16] the reflection−absorption absorbance, A_R, is given by

$$A_R = 2m_z \cos^2 \alpha + m_x \sin^2 \alpha$$

where α is the angle between the transition moment and the normal direction of a surface and m_z and m_x are the intensity enhancement factors of the normal and surface compoments of the extinction coefficients due to the substrate surface. In the present studies, an accurate angle, α, was not calculated because m_z and m_x were not reported for a silicon wafer. If the surface of the silicon wafer acts as a semiconductor substrate, m_z is much larger than m_x, leading to the well-used approximation

$$A_R = 2m_z \cos^2 \alpha$$

According to this equation, the intensity increases as the transition moment takes a more perpendicular direction from the substrate surface. As for the orientation of the CH groups in the Ru(II) complex, the groups are assumed to be oriented uniformly in all directions since 18 CH groups are located on the periphery region of the spherically shaped Ru(II) complex in different directions. Thus, the peaks at 1106 cm^{-1} would not show any orientational effect in both the racemic and enantiomeric films. On the basis of these situations, we assume that the intensity of the peak at 1106 cm^{-1} may be taken as a normalizing factor in estimating the relative intensities of other peaks. On the basis of this assumption, the ratios of the peak intensities of the CH_2 groups of SA molecules (2700−2800 cm^{-1}) to that of CH groups in the dpp ligands (1106 cm^{-1}) are calculated and given in Table 2. The results indicate that the transition moments of the symmetric and asymmetric stretching vibrations of the CH_2 groups in the LB films are more perpendicular for the enantiomeric film than for the racemic film. Because these transition moments are perpendicular to the alkyl chain, it is deduced that the alkyl chain of SA has a more upright direction for the racemic mixture than for the enantiomer. In contrast, the difference of the relative intensities between the racemic and enantiomeric cast films was much

TABLE 2: Relative Intensities of the IR Peaks Due to the CH_2 Stretching of the Alkyl Chains of Stearic Acid Incorporated in the LB and Cast Films of 1:1 $[Ru(dpp)_3]^{2+}$ and Stearic Acid According to the Results in Figures 9 and 10[a]

film	peak position (cm^{-1})	assignment	racemic mixture	enantiomer
LB	2923	asym. stretching of CH_2	0.589	3.00
	2854	sym. stretching of CH_2	0.333	2.00
	1106	out-of-plane bending of CH	1.00	1.00
cast	2917	asym. stretching of CH_2	0.704	0.860
	2848	sym. stretching of CH_2	0.481	0.672
	1118	out-of-plane bending of CH	1.00	1.00

[a] The intensity of the peak due to the out-of-plane bending vibration of CH groups is taken to be unity in each film.

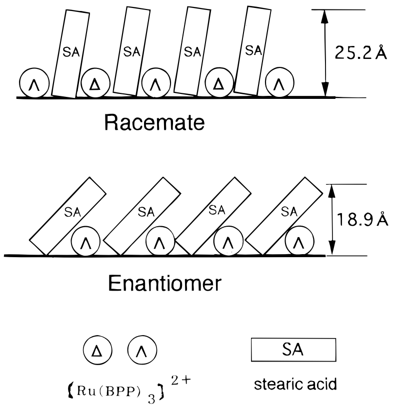

Figure 11. Proposed structures of the monolayers of $[Ru(dpp)_3](ClO_4)_2$ and stearic acid at [Ru]/[SA] = 1: (a) racemic mixture and (b) enantiomer.

smaller than in the LB films. This indicates that the SA molecules have a more random orientation in the cast films irrespective of homo- and heterochirality.

We rationalize the above results in terms of the following packing models. In the enantiomeric film, metal complexes and stearate anions form a mixed layer in which stearate anions intervene in metal complexes, whereas in the racemic film, stearate anions take a more upright direction because the racemic metal complexes are so closely packed that there is less room left for stearate anions. Our packing model is schematically shown in Figure 11.

The presence of a phase transition was possible for the racemic mixture at [SA]/[Ru] = 2 (Figure 4). When chiral molecules form a two-dimensional crystal, the racemic mixture is expected to have a larger number of packing states than the enantiomer.[7] The situation is most remarkable when the crystal takes an oblique lattice.[7] In this case, the racemic mixture has two diastereomeric lattices, whereas the enantiomer has a single lattice. The phase transition observed in Figure 4 may be related to the transition of the racemic mixture between these phases.

The stereochemical effects observed herein may provide a way to control the packing of amphiphilic molecules in a molecular layer by the use of molecular chilarity.[16,23]

References and Notes

(1) Roberts, G. G. *Adv. Phys.* **1985**, *34*, 475−512 and references therein.

(2) Richardson, T.; Roberts, G. G. *Thin Solid Films* **1988**, *160*, 231−239.

(3) Richardson, T.; Roberts, G. G.; Polywka, M. E. C.; Davies, S. G. *Thin Solid Films* **1989**, *179*, 405−411.

(4) Poulter, M. W.; Roberts, G. G.; Costello, J. F.; Davies, S. G.; Edwards, A. J. *Thin Solid Phys.* **1992**, *210/211*, 427−429.

(5) Sprintschnik, G.; Sprintschnik, H. W.; Kirsh, P. P.; Whitten, D. G. *J. Am. Chem. Soc.* **1976**, *98*, 2337−2338.

(6) Sakaguchi, H.; Gomez-Jahn, L. A.; Prichard, M.; Penner, L. T.; Whitten, D. G.; Nagamura, T. *J. Phys. Chem.* **1993**, *97*, 14474−1476.

(7) Eckhart, C. J.; Peachey, N. M.; Swanson, D. R.; Takacs, J. M.; Khan, M. A.; Gong, X.; Kim, J. H.; Wang, J.; Uphous, R. A. *Nature* **1993**, *362*, 614−616.

(8) Lundquist, M. *Ark. Kemi* **1960**, *17*, 183−195.

(9) Lundquist, M. *Ark. Kemi* **1962**, *21*, 395−406.

(10) Lundquist, M. *Ark. Kemi* **1963**, *23*, 299−306.

(11) Tachibana, T.; Yoshizumi, T.; Hori, K. *Bull. Chem. Soc. Jpn.* **1979**, *52*, 34−41.

(12) (a) Heath, J. G.; Arnett, E. M. *J. Am. Chem. Soc.* **1992**, *114*, 4500. (b) Arnett, E. M.; Harvey, N. G.; Rose, P. L. *Acc. Chem. Res.* **1989**, *22*, 131−138 and references therein.

(13) Miller, C. J.; McCord, P.; Bard, A. J. *Langmuir* **1991**, *7*, 2781−2787.

(14) Samha, H.; DeArmond, M. K. *Langmuir* **1994**, *10*, 4157−4163.

(15) Clark, G. L.; Leppla, P. W. *J. Am. Chem. Soc.* **1936**, *58*, 2199−2201.

(16) Umemura, J.; Kamata, T.; Kawai, T.; Takenaka, T. *J. Phys. Chem.* **1990**, *94*, 62−67.

(17) Mason, S. F. *Molecular Optical Activities and the Chiral Discriminations*; Cambridge University Press: Cambridge, 1982; pp 169−175.

(18) Kuroda, R.; Mason, S. F. *J. Chem. Soc. Dalton* **1979**, 273.

(19) Kobayashi, H.; Matsuzawa, H.; Kaizu, Y.; Ichida, A. *Inorg. Chem.* **1987**, *26*, 4318−4323.

(20) Morosin, B. *Acta Crystallogr.* **1963**, *19*, 131−137.

(21) Masuda, Y.; Yamatera, H. *Bull. Chem. Soc. Jpn.* **1984**, *57*, 58−62.

(22) Andelman, D. *J. Am. Chem. Soc.* **1989**, *111*, 6536−6544.

(23) Dhenaut, C.; LeDoux, I.; Samuel, I. D. W.; Zyss, J.; Bourgault, M.; Le Bozex, H. *Nature* **1995**, *374*, 339−342.

JP952181A